UNSTEADY INVESTIGATION OF THE DLR TIC NOZZLE BY DIFFERENT TURBULENCE MODELS ATAC – TEST CASE 1C

Heinrich Luedeke
DLR, Institute of Aerodynamics and Flow Technology
Lilienthalplatz 7, D-38108 Braunschweig

1. Introduction

Afterbodys of launchers and re-entry vehicles are characterized by large base regions submitted to intense back flow, aerodynamic instabilities and pressure fluctuations on the afterbody and on the nozzle region. Consequently in addition to experimental investigations a necessary capability of numerical tools is the capability to simulate unsteady super- and hypersonic flow fields of such configuration and to resolve turbulent wake flows, interacting with nozzle sections, on realistic launcher configurations.
One of the experimental activities in this scope was performed by DLR at the P6.2 facility in Lampoldshausen [1], Germany, providing an experimental data base for the DLR TIC nozzle under overexpanded cold gas conditions (Fig. 1). Key objectives of this test case are the correct prediction of the separation location and the assessment of the resulting unsteady side load torque. The geometry was specified by DLR, including nozzle inner and outer wall and the inflow geometry upstream the nozzle throat.
The present computations were performed as a feasibility study, end preliminary results are presented here.Different computations on unstructured grids were carried out with grid adaptation at the shock structures. The test case was investigated by different descriptions of the turbulent flow field such as one equation URANS models and a DES (Detached Eddy Simulation) type simulation as well as laminar conditions. It has to be pointed out that the investigated grids are too coarse for a realistic DES and the resulting turbulence is only insufficiently resolved. Nevertheless the behaviour of the model under these conditions had to be investigated to earn experience for further simulations.

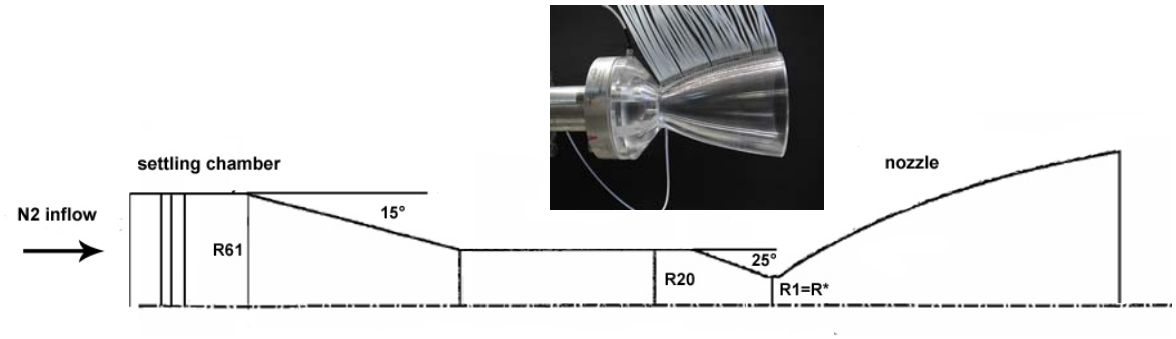

Fig. 1 Test case geometry and experimental set-up in the P6 facility at DLR Lampoldshausen.

2. Numerical tools

The presented investigation was carried out using the hybrid structured/unstructured DLR-Navier-Stokes solver TAU, which is validated for a wide range of steady and unsteady sub- trans- and hypersonic flow cases [1].
TAU is a second order finite-volume flow solver for the Euler and Navier-Stokes equations in the integral form. Different numerical schemes like cell-centred for sub- and transonic flow and AUSMDV for super- and hypersonic flow conditions are implemented. Second-order accuracy for upwind schemes is obtained by the MUSCL extrapolation in order to allow the capturing of strong shocks and contact discontinuities. A three-stage Runge-Kutta scheme and an implicit LUSGS scheme as additional option is implemented to advance the solutions in time for steady flow fields. For acceleration of the convergence local time stepping, implicit residual smoothing and full multigrid are available.
For time efficient and accurate transient flow simulations a dual time stepping scheme, following Jameson is implemented, which is an implicit algorithm and not related to the choice of the smallest timestep in the flow field. To overcome this limit the time derivative in the Navier-Stokes equations is

discretized by a second order backwards difference, resulting in a non-linear equation system which converges towards the subsequent timestep by using an inner pseudo-time. With this approach the performance of time accurate computations can be accelerated by 2-3 orders of magnitude.
Several one- and two equation turbulence models are available for steady simulations. In the presented RANS-cases the one-equation Spalart-Allmaras (SA) model is used which is described in detail in [3].
During the last years modern turbulence models like DES are implemented [4][5][6]. DES is a hybrid RANS-LES approach that is based on a modification of the wall distance term in the SA model. While RANS is used in the unsteady boundary layer flow where it provides reasonable results, LES is used in separated regions where relevant turbulent scales are modelled. The switching between RANS and LES bases on a characteristic length scale, chosen to be proportional to the largest cell dimension Δ.
For the standard DES formulation the wall distance d in the SA model is replaced by $\tilde{d}$, defined as:

$$\tilde{d} = \min(d, C_{DES}\Delta) \tag{7}$$

with C_{DES} as a constant calibrated by using isotropic turbulence. In this mode a local equilibrium between the production and the destruction term in the SA model is expected. This local balance leads to the relation $\tilde{\nu} \propto \tilde{S} \cdot \tilde{d}^2$ with $\tilde{\nu}$ denoting the modified eddy viscosity in the Spalart Allmaras model and $\tilde{S}$ the modified shear stress tensor. This relation is similar to the Smagorinsky LES model. Therefore this modified RANS model represents an LES formulation outside the boundary layer.

3. Grids and flow conditions

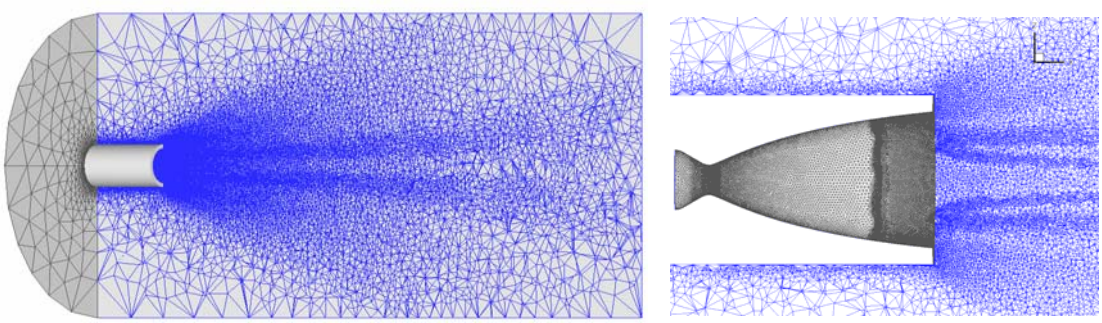

Fig. 2 Symmetry plane of the generic configuration and surface grid distribution on the nozzle wall of the three times adapted grid.

The investigated test case was using an ambient pressure of 1 bar at a temperature of 300 K in the far field. For the experiments kold nitrogen at a chamber pressure of 33.5 bar and a feeding temperature of 300 K was in use. The flow conditions for the simulation were chosen fully turbulent with an inflow velocity of 10 m/s.

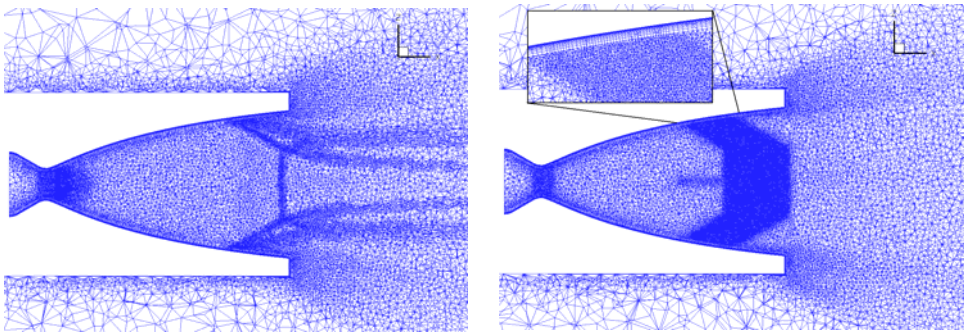

Fig. 3 Symmetry plane of adapted grid inside the nozzle (left) and pre-refined grid in the shock region and boundary layer (right).

Different unstructured grids were generated for the configuration. The basic grid is shown in Fig. 2. It is pre-refined approximately to resolve the expected flow structures. Further grid adaptation was performed in the course of the computation. This was especially necessary for the shock system as shown in Fig. 3. For a better resolution of shear instabilities further improved grids were generated (Fig. 3 right).

4. Steady SA-RANS results

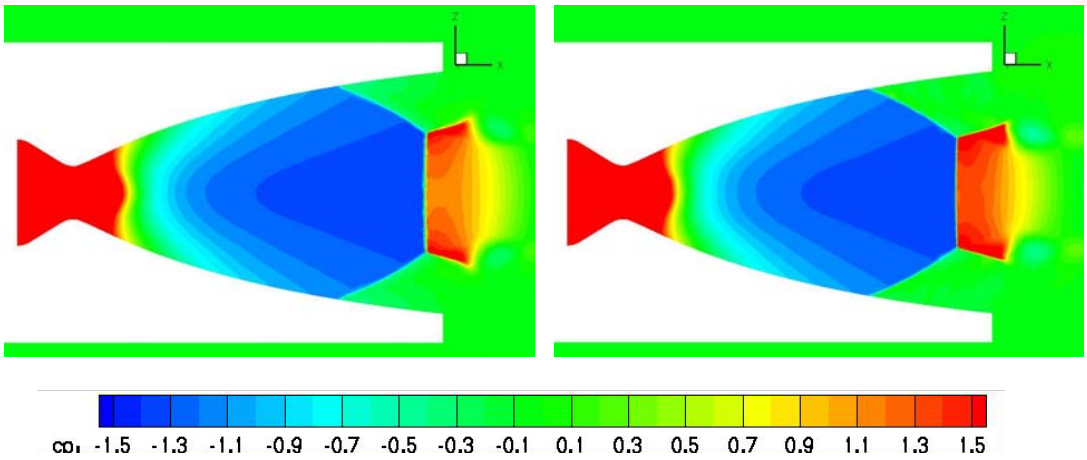

Fig. 4 Cp distribution inside the nozzle, resulting from SA-RANS computations, left: on adapted grid, right on pre-refined grid

As a first step, steady RANS simulations of the flow field where carried out on the generated grids. The results on the three times adapted grid (Fig. 4 left) and the pre-refined grid (Fig. 4 right) are nearly identical in the pressure distribution. As expected the shock inside the nozzle is approximately straight without indication of re-circulation downstream. This was not the case for the unadapted basic grids where a shock curvature was clearly visible (not shown here). The reason for this grid dependency can be found in the necessity, that the flow behind the shock has to match the shear layer flow and consequently the stream lines have to be bent behind the shock. For this bending a sufficient number of cells are necessary downstream of the shock which is only the case on sufficiently refined grids.

5. Unsteady laminar and turbulent results

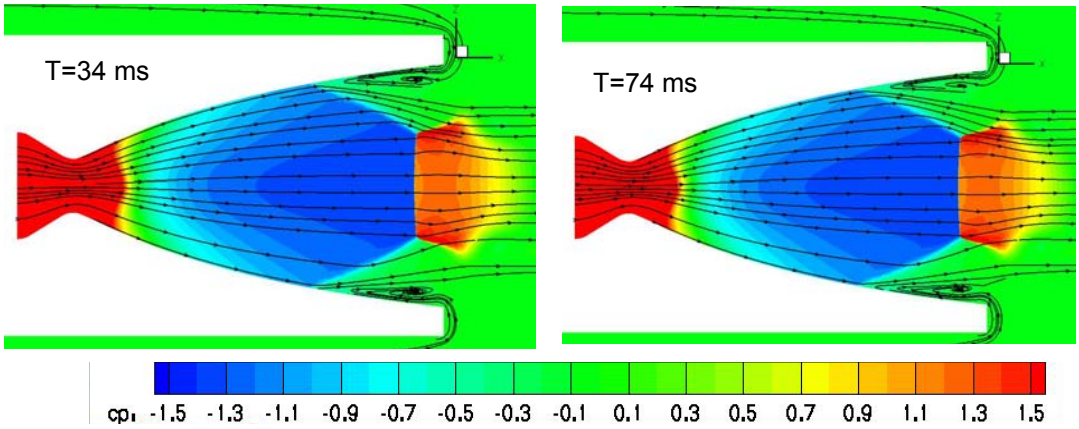

Fig. 5 URANS results on unsteady adapted grids at T=34 ms (left) and T=74 ms (right) (ΔT=0.5 ms).

The steady results, described in the previous section, are used as start solutions for unsteady computations with the SA one equation model. The grids where adapted by moving to the new shock position every fifth time step at a time step size of 0.5 ms which was chosen based on the size of the re-circulation bubble and the velocity in this region. This solution reveals steady behaviour after very few adaptations and consequently nearly no side forces are computed.
In Fig. 5 the pressure distribution and the flow topology shows a fully symmetric behaviour. Behind the shock the stream lines are bent without re-circulation as already described in section 4. Near the wall

the free shock separation with a re-circulation zone appears. Even this usually highly unstable flow structure is nearly symmetric and steady.
A first possible explanation for this behaviour, is the well known overestimation of the turbulent viscosity in the free shear layer and the separation zone by the standard Spalart Allmaras model. To check this hypothesis fully laminar computations with the same time step where carried out, despite of the fact, that the re-circulation bubble will be obviously by far too large. In fact the unsteadiness of the resulting side forces is stronger for laminar conditions, but still ten times lower than the measured loads. In Fig. 6 the asymmetries that result in additional side loads can be seen especially in the lower separation. This effect vanishes after 160 ms (Fig. 6 right). Flow separation behind the shock is visible in this case, due to the insufficient grid resolution in this region.
To reduce the eddy viscosity in the shear layer another simulation was started on a pre-refined grid by using DES. It was already pointed out, that the grids are to coarse for a sufficient resolution of relevant turbulent structures. The only advantage of the technique, using the present grids, is the described behaviour of the eddy viscosity. In fact the separation point was found at the correct position, however no significant unsteadiness could be observed after a sufficient number of physical time steps.

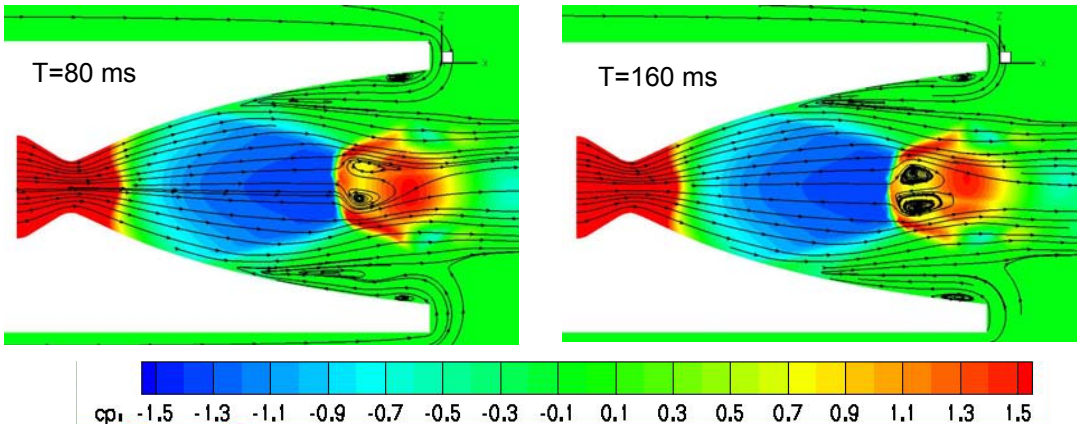

Fig. 6 Unsteady laminar results after 80 and 160 ms on the basic unadapted grid.

6. Specific flow features

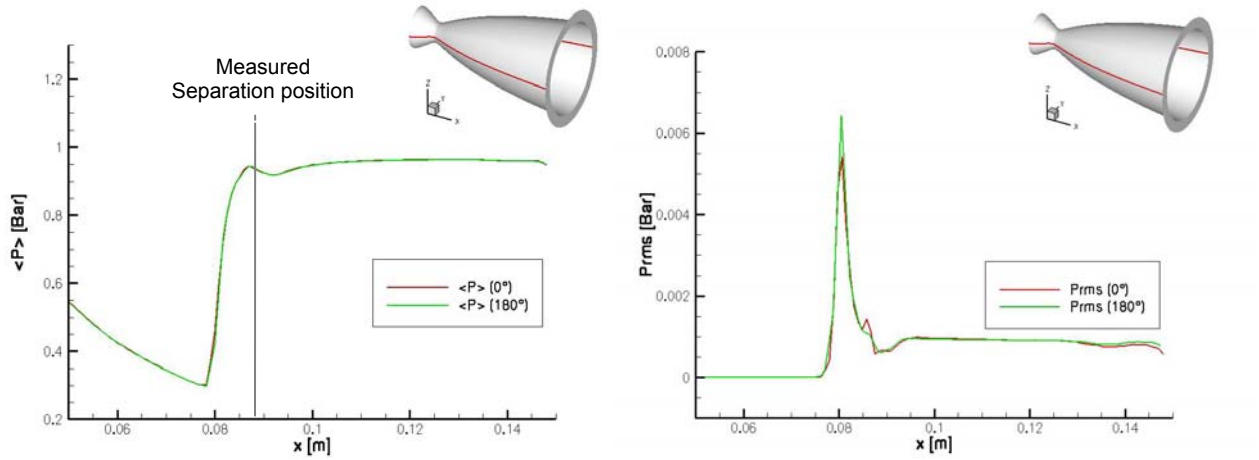

Fig. 7 Averaged wall pressure and RMS pressure distribution in the separated region.

To get insight into the flow structure and to derive reasons for the behaviour of the simulations, pressure distributions and root mean square (RSM) distributions are determined on a line along the nozzle wall. The curves in Fig. 7 show a slightly larger separation position than the measured one at 0.088m. The distribution of the RMS values has the correct shape if compared with the data of Deck [7], but its magnitude by far too small. The time developments of the side load torque in Fig. 8 show typical characteristics of a damped oscillator. This provides an indication of a perturbed shock position due to the start conditions which is vanishing with time. The non symmetry of the moments is a result of the unstructured grid, which is never fully symmetric.

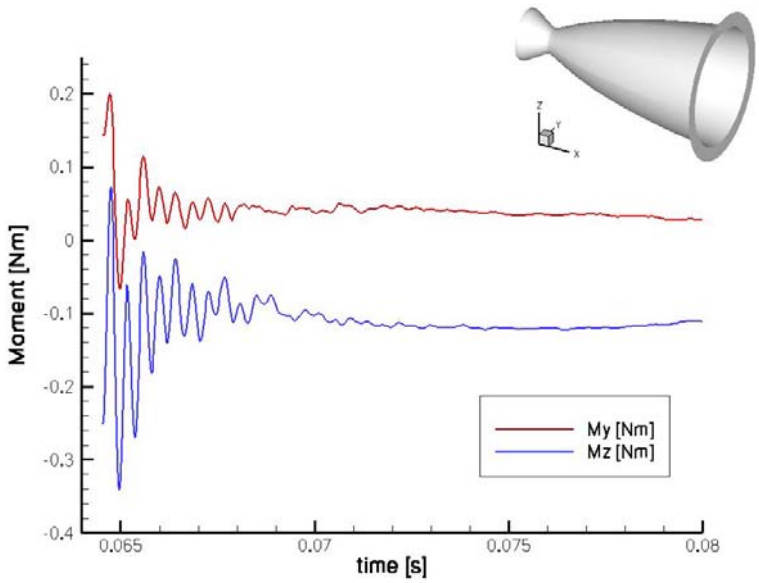

Fig. 8 Side load torque as a function of time for a turbulent solution during the startup phase of the simulation.

One reason for the steadiness of the solutions is found in the startup conditions which were not chosen by the physical background of the experiment, but by the intention to stabilize the computation during the unconverged transient phase. Consequently up to here all computations were stated by initializing the flow field with transonic free stream conditions. To test the hypothesis of the necessity to re-create the experimental conditions also for the startup, a new computation was carried out, initialized by total conditions and zero velocity. A first unconvered result is shown in Fig. 9. First instabilities in the plume are visible and larger side loads appear. These simulations are still running and will be continued.

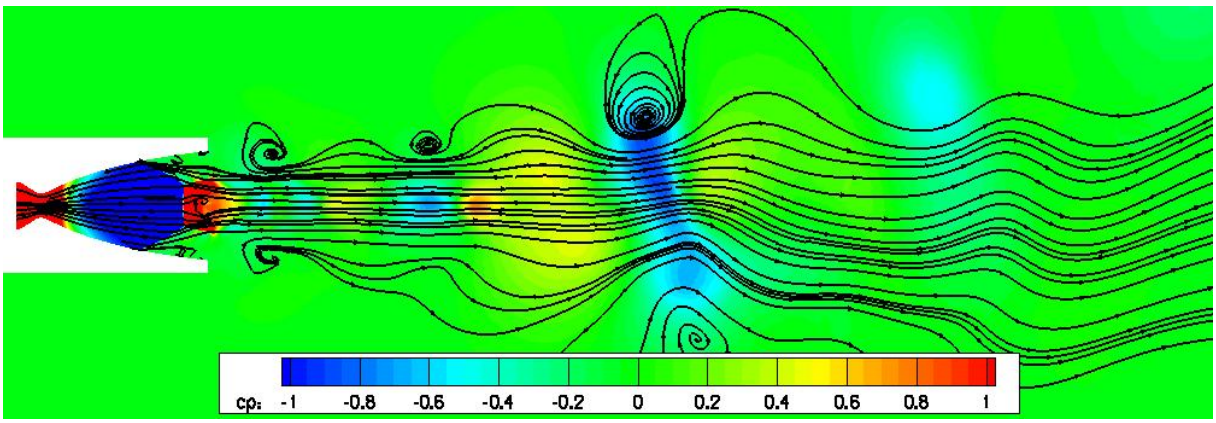

Fig. 9 influence of the start condition: unconverged result after 3000 iterations, started from total conditions.

Another reason for an unsteady mixing in the plume, especially in the circumferential direction, is the appearance of streamwise counter-rotating vortices. These are amplified instabilities which develop due to the concave shape of the nozzle in the separation zone (see [8]). This instability is visualized in Fig. 10 in three cuts behind the nozzle outflow plane. After 3000 iterations, these structures are still non-regular and a mixing over the whole cross section is possible. 1500 iterations later, the structures are nearly regular and the computation becomes steady, since no mixing from one zone of a vortex pair into another is possible. From the physical point of view for an unsteady solution no regularity is expected, but a chaotic mixing in circumferential direction. A consequence of this observation would be the implementation of disturbance velocities in circumferential direction.

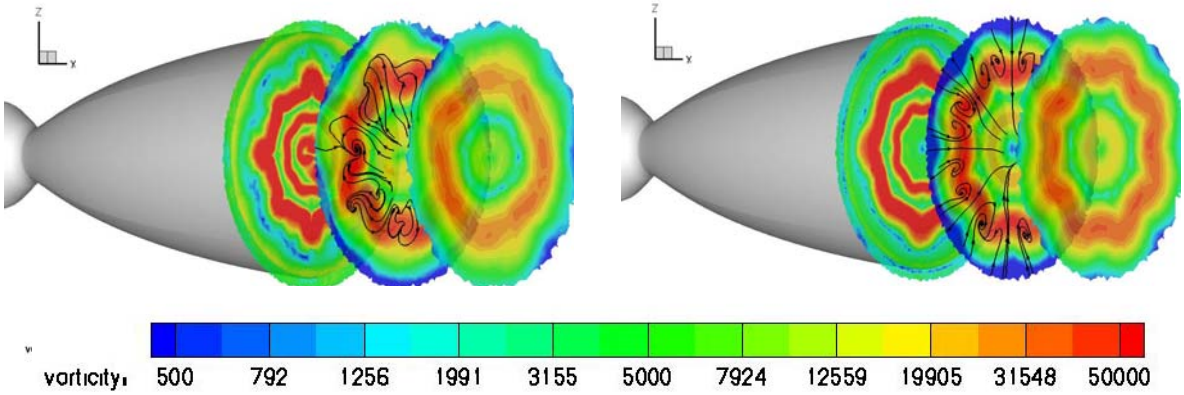

Fig. 10 Cut planes behind the nozzle showing vorticity. Left: after 3000 iterations, right: after 4500 Iterations.

7. Conclusion

In the present study an over-expanded DLR TIC nozzle was investigated using the DLR TAU code. Simulations were carried out on different adapted and pre-refined grids with similar results and nearly identical separation points. The shape of the mach disk as a plane shock structure without recirculation downstream was well predicted after adaptation. Different techniques of turbulence modelling are tested as well as laminar computations, where the separation for the latter one was by far too large as expected. In all cases steady solutions were obtained after some iterations, though in laminar cases more unsteadiness was investigated. Plots of the unsteady side load torque show the typical behaviour of a perturbed linear oscillator, which is a well known response of the shock system. For all cases the numerically predicted side loads are more or less steady in contrast to the experimental results. Further studies with smaller time steps should overcome this problem at least gradually. First computations with changed parameters are quite promising.

References

[1] M. Frey: Behandlung von Strömungsproblemen in Raketendüsen bei Überexpansion. Institut für Aerodynamik und Gasdynamik der Universität Stuttgart, http://elib.uni-stuttgart.de/opus/volltexte/2001/800/, (2001)

[2] A. Mack, V. Hannemann: Validation of the unstructured DLR-TAU-Code for Hypersonic Flows, AIAA 2002-3111, (2002).

[3] P.R. Spalart, S.R. Allmaras: A One Equation Turbulence Transport Model for Aerodynamic Flows, La Recherche Aérospaciale, No. 1, 1994, pp. 5-21.

[4] P.R. Spalart: Young-Person's Guide to Detached- Eddy Simulation Grids. NASA/CR-2001-211032, (2001).

[5] H. Lüdeke, A. Filimon: Investigations of Transient Flow Phenomena at the ARIANE-5 Propulsion System During Ascent. 5th European Symposium on Aerothermodynamics for Space Vehicles, Cologne, November 8-11 (2004).

[6] H. Lüdeke, A. Filimon: Time Accurate Simulation of Turbulent Nozzle Flow by the DLR TAU-code. 14th DGLR STAB Symposium, Bremen, November 16-18 (2004).

[7] S. Deck, P.Guillen: Numerical Simulation of Side Loads in an Ideal Truncated Nozzle. 14th Journal of Propulsion and Power, Vol. 18, No. 2, 261-269 (2002).

[8] H. Lüdeke: Untersuchung von Längswirbeln in abgelösten hypersonischen Strömungen. DLR Forschungsbericht 2003-04 (2003)